The bZIP1 Transcription Factor Regulates Lipid Remodeling and Contributes to ER Stress Management in *Chlamydomonas reinhardtii*

Yasuyo Yamaoka, Seungjun Shin, Bae Young Choi, Hanul Kim, Sunghoon Jang, Masataka Kajikawa, Takashi Yamano, Fantao Kong, Bertrand Legeret, Hideya Fukuzawa, et al.

The bZIP1 Transcription Factor Regulates Lipid Remodeling and Contributes to ER Stress Management in *Chlamydomonas reinhardtii*

Yasuyo Yamaoka[1]*, Seungjun Shin[1], Bae Young Choi[1], Hanul Kim[2], Sunghoon Jang[2], Masataka Kajikawa[3], Takashi Yamano[3], Fantao Kong[4], Bertrand Légeret[4], Hideya Fukuzawa[3], Yonghua Li-Beisson[4], Youngsook Lee[1,2]*

[1]Department of Integrative Bioscience & Biotechnology, POSTECH, Korea,
[2]Department of Life Science, POSTECH, Korea,
[3]Graduate School of Biostudies, Kyoto University, Japan,
[4]Aix Marseille Univ, CEA, CNRS, BIAM, Saint Paul-Lez-Durance, France.
*Corresponding authors: Yasuyo Yamaoka, Department of Integrative Bioscience & Biotechnology, POSTECH, Pohang 790-784, Korea (Tel +82 54 279 8373; fax +82 54 279 2199; email yamaoka1982@postech.ac.kr), Youngsook Lee, Department of Life Science, POSTECH, Pohang 790-784, Korea (Tel +82 54 279 2296; fax +82 54 279 2199; email ylee@postech.ac.kr).

E-mail addresses of all authors:
Yasuyo Yamaoka, yamaoka1982@postech.ac.kr; Seungjun Shin, shine5639@postech.ac.kr; Bae Young Choi, baeyoung@postech.ac.kr; Hanul Kim, hanulkim@postech.ac.kr; Sunghoon Jang, hecj@postech.ac.kr; Masataka Kajikawa, kajikawa@lif.kyoto-u.ac.jp; Takashi Yamano, tyamano@lif.kyoto-u.ac.jp; Fantao Kong, kongfantaohit@163.com; Bertrand Légeret, Bertrand.legeret@cea.fr; Hideya Fukuzawa, fukuzawa@lif.kyoto-u.ac.jp; Yonghua Li-Beisson, yonghua.li@cea.fr; Youngsook Lee, ylee@postech.ac.kr.

The authors declare there is no conflict of interests.

Running title: CrbZIP1 modulates membrane lipids under ER stress

One-Sentence Summary: The mRNA of a *Chlamydomonas* bZIP transcription factor is spliced by CrIRE1 under ER stress, and the resulting protein protects *Chlamydomonas* cells from ER stress by modulating lipid remodeling.

Keywords: bZIP; Chlamydomonas; DGTS; ER stress; pinolenic acid

Word count: 7958 words

ABSTRACT

Endoplasmic reticulum (ER) stress is caused by the stress-induced accumulation of unfolded proteins in the ER. Here, we identified proteins and lipids that function downstream of the ER stress sensor inositol-requiring enzyme1 (CrIRE1), which contributes to ER stress tolerance in *Chlamydomonas reinhardtii*. Treatment with the ER stress inducer tunicamycin resulted in the splicing of a 32-nucleotide fragment of a bZIP transcription factor (*CrbZIP1*) mRNA by CrIRE1, which resulted in the loss of the transmembrane domain in CrbZIP1, and the translocation of CrbZIP1 from the ER to the nucleus. Mutants deficient in *CrbZIP1* failed to induce the expression of the unfolded protein response genes and grew poorly under ER stress. Levels of diacylglyceryltrimethylhomo-Ser (DGTS) and pinolenic acid (18:3Δ5,9,12) increased in the parental strains but decreased in the *crbzip1* mutants under ER stress. A yeast one-hybrid assay revealed that CrbZIP1 activated the expression of enzymes catalyzing the biosynthesis of DGTS and pinolenic acid. Moreover, two independent alleles of *crdes* mutant, which failed to synthesize pinolenic acid, were more sensitive to ER stress than were their parental lines. Together, these results indicate that *CrbZIP1* is a critical component of the ER stress response mediated by CrIRE1 in *Chlamydomonas* that acts via lipid remodeling.

INTRODUCTION

Chlamydomonas reinhardtii is a model microalga widely used for studies of photosynthesis, flagella biogenesis, and lipid metabolism (Harris, 2001). Similar to many other microalgae, *Chlamydomonas* produces a large amount of triacylglycerol (TAG) under stress conditions (Merchant et al., 2012), and this prompted intensive studies of the mechanisms underlying stress responses in this organism. The endoplasmic reticulum (ER) stress response is an important stress response that is common to many eukaryotes. ER stress can be induced by biotic and abiotic factors, such as pathogen infection, temperature, high salinity, wounding, and ER stress inducing agents (Howell, 2013), and results in the accumulation of unfolded proteins in the ER. In mammals, the unfolded proteins accumulated in the ER are sensed by proteins in the ER membrane that transmit this information to the nucleus, inducing the expression of genes and restoring normal protein metabolism. This process is called the unfolded protein response (UPR). UPR genes encode molecular chaperones, folding enzymes, lipid biosynthesis enzymes, and components of the ER-associated protein degradation pathway (Ron and Walter, 2007).

Recently, lipid metabolism was also found to be altered in many types of cells exposed to ER stress. In animal cells, ER stress increases *de novo* lipogenesis and TAG accumulation (reviewed in Basseri and Austin 2012; Mandl et al 2013; Zhou and Liu 2014; Han and Kaufman 2016). In animal and yeast cells, exposure to ER stress promotes the biosynthesis of phosphatidylcholine (PC), a major ER membrane lipid, expanding the ER membrane area (Sriburi et al., 2007; Schuck et al., 2009) and thereby attenuating the damage caused by the stress. The biosynthesis and storage of TAG in lipid droplets might also ameliorate the damage caused by various stress conditions, since stress often leads to the degradation of membrane lipids and the release of free fatty acids to toxic levels (Listenberger et al., 2003). However, little is known about the changes in other lipid molecules that occur during ER stress. Thus, it would be useful to determine the entire lipid profile of a cell, to monitor how it changes in response to ER stress, and to establish how it differs in mutants that do not have a normal ER stress response.

The *C. reinhardtii* genome encodes only one ER stress sensor, i.e., inositol-requiring enzyme 1 (CrIRE1). IRE1 is the best conserved ER stress sensor among metazoans, yeast, and plants (Yamaoka et al., 2018). IRE1 is a dual-function protein that has both kinase and ribonuclease (RNase) activity. Under ER stress, IRE1 dimerizes and then auto-phosphorylates, triggering its RNase activity. Active IRE1 splices mRNA encoding a

transcription factor named *Hac1* in budding yeast, *XBP1* (*X-box binding protein-1*) in metazoans, and *bZIP60* in *Arabidopsis thaliana* (Kimata and Kohno 2011; Ron and Walter, 2007; Howell, 2013).

CrIRE1 plays an essential role in ER stress tolerance in *Chlamydomonas*, similar to IRE1s of other organisms, but differs from other IRE1s in the C-terminal tandem zinc-finger domain (Yamaoka et al., 2018). The conserved kinase and RNase domains of CrIRE1 suggest that CrIRE1, like other IRE1 proteins, splices the mRNA of a transcription factor; however, the identity of this transcription factor was hitherto unknown in *Chlamydomonas*.

In this study, we identified a transcription factor, CrbZIP1, that governs the ER stress response in *Chlamydomonas*, and revealed the underlying molecular mechanism. In addition to providing insight into the mode of action of CrbZIP1, this study highlights the importance of membrane lipid remodeling in ER stress management.

RESULTS

Chlamydomonas bZIP1 mRNA is spliced under ER stress

We searched for the mRNA targeted by CrIRE1 from among *Chlamydomonas* basic leucine zipper (bZIP) proteins, since IRE1 proteins of diverse organisms activate bZIP transcription factors by splicing their mRNA (Kimata and Kohno 2011; Ron and Walter, 2007; Howell, 2013). Among the 19 genes that contain a bZIP domain in the *Chlamydomonas* genome, we decided to study Cre05.g238250 (CrbZIP1) as the potential target gene of CrIRE1, as it was the closest relative of Arabidopsis AtbZIP60 (Figure 1A), the established target of AtIRE1 (Nagashima et al., 2011; Deng et al., 2011).

To test whether *CrbZIP1* was indeed the target gene of CrIRE1, we first tested whether the *CrbZIP1* transcript was spliced under ER stress conditions. Under normal conditions, there was only one product of *CrbZIP1* transcription, but under the ER stress induced by tunicamycin, there were two different *CrbZIP1* transcripts in the *Chlamydomonas* strains CC-4533 (*cw15 mt*$^-$, cell wall-deficient) and C-9 (CC-5098, *mt*$^-$) (Figure 1B). However, in the CrIRE1 knock-down mutants *crire1-1* and *crire1-2*, whose parental strain is CC-4533 (Yamaoka et al., 2018), the smaller transcript was barely detectable (Figure 1B). Sequencing of the transcripts revealed that 32 nucleotides were spliced out of the *CrbZIP1* transcript under ER stress, resulting in a frameshift and generating a new stop codon (Figure 1C). We designated the un-spliced form of *CrbZIP1* as *CrbZIP1u* and the spliced form of *CrbZIP1* as *CrbZIP1s*. The conserved nucleotide sequence commonly found at the splicing site in the stem-loop structure of IRE1-target mRNA (*AtbZIP60, HAC1, XBP1* shown in Supplemental Figure 1) did not exist in the double stem-loop of *CrbZIP1* mRNA predicted using CentroidFold (Supplemental Figure 1 *CrbZIP1*; http://rtools.cbrc.jp/centroidfold/), suggesting that *Chlamydomonas* IRE1 uses a different mechanism to recognize and splice the target mRNA.

We then compared the predicted structures of proteins encoded by CrbZIP1u and CrbZIP1s. Both were predicted to contain a bZIP domain, but only CrbZIP1u contained a transmembrane domain (Figure 1D). The new stop codon generated by splicing was predicted to delete the transmembrane domain (Figures 1C and 1D). In *Arabidopsis*, *AtbZIP60* mRNA is spliced by IRE1A/IRE1B at the site of the double stem-loop structure (Supplemental Figure 1), which causes a frameshift and consequent deletion of a transmembrane domain in AtbZIP60 (Nagashima et al., 2011; Deng et al., 2011). Then, the transcription factor is no longer located at the ER membrane, but enters the nucleus and regulates the expression of ER-stress-related genes. To test whether CrbZIP1 undergoes similar modification under ER

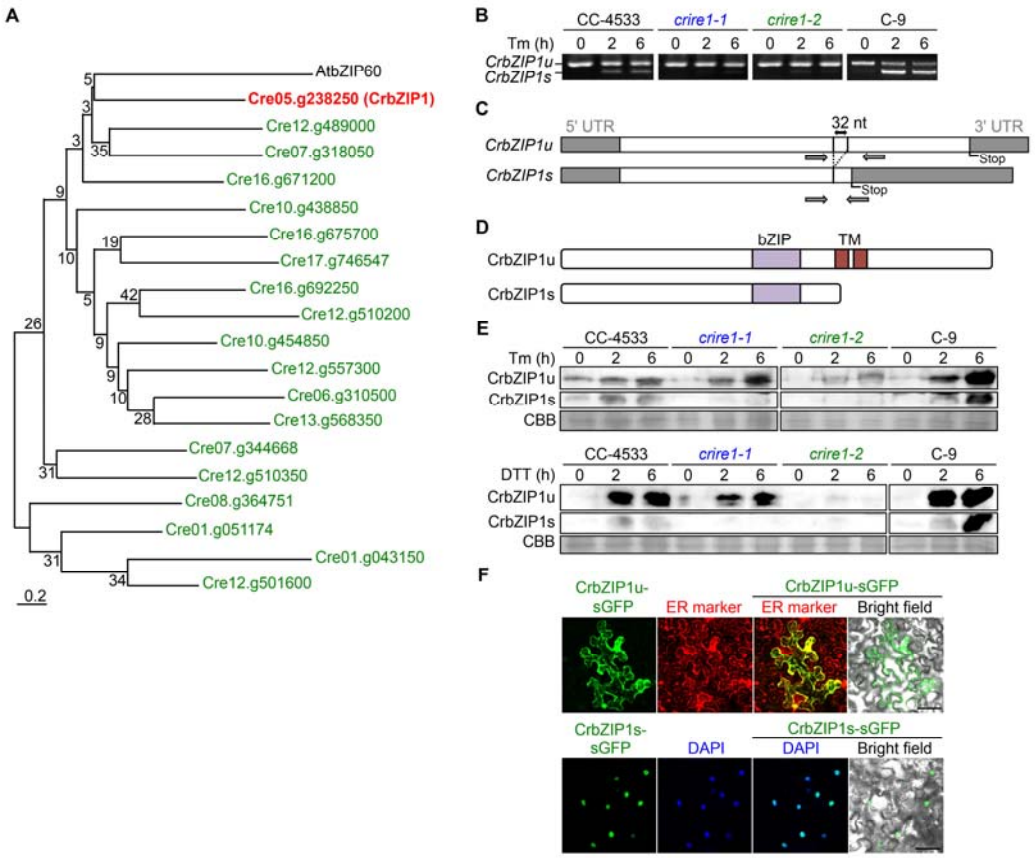

Figure 1. Identification of the transcription factor targeted by *Chlamydomonas* IRE1.
(**A**) Molecular phylogenetic analysis of the *Chlamydomonas* bZIP proteins and the *Arabidopsis* AtbZIP60 protein reported to be important for ER stress (Nagashima et al., 2011; Deng et al., 2011). The analysis was conducted in MEGA7 (Kumar et al., 2016), using the Maximum Likelihood method based on the JTT matrix-based model (Jones et al., 1992). The tree is drawn to scale, with branch lengths measured in number of substitutions per site.
(**B**) Unspliced *CrbZIP1* (*CrbZIP1u*) and spliced *CrbZIP1* (*CrbZIP1s*) detected using primers flanking the spliced region of *CrbZIP1* (arrows in C). Under the ER stress conditions imposed by 1 μg/mL tunicamycin (Tm), *CrbZIP1u* is spliced to *CrbZIP1s* in CC-4533 and C-9, but not in the *crire1* mutants, *crire1-1* and *crire1-2*. *Chlamydomonas* cells were incubated in TAP medium containing 1 μg/mL Tm.
(**C**) Schematic representations of *CrbZIP1u* mRNA and *CrbZIP1s* mRNA and primer locations used to detect splicing.
(**D**) Schematic representations of primary structures of CrbZIP1u and CrbZIP1s proteins. The bZIP motif and the transmembrane domain are indicated by bZIP and TM, respectively.
(**E**) Immunoblot analysis of CrbZIP1u and CrbZIP1s using anti-CrbZIP1 antibody. Protein preparations from cells treated with 1 μg/mL tunicamycin (Tm) or 5 mM dithiothreitol (DTT) for the indicated periods were subjected to immunoblot analysis. Coomassie brilliant blue staining (CBB) was used as a loading control.
(**F**) Cellular localization of CrbZIP1u-sGFP and CrbZIP1s-sGFP transiently expressed in *N. benthamiana* epidermal cells. The superfolder GFP (sGFP), ER marker (AtBiP1-tagRFP), DAPI (nuclear marker), and merged images of sGFP and ER marker, DAPI, and the bright field. Note that CrbZIP1u-sGFP mainly localizes to the ER membrane and CrbZIP1s-sGFP localizes to the nucleus. Typical images of each localization pattern were chosen from each of the 6 images analyzed. Bars = 50 μm.

stress, we analyzed the size and amount of CrbZIP1u and CrbZIP1s proteins under normal conditions and the ER stress conditions induced by treatment with 1 μg/mL tunicamycin by immunoblotting with anti-CrbZIP1 antibody (Figure 1E, Supplemental Figure 2A). Under normal conditions, CrbZIP1 protein bands were barely detectable, but after ER stress treatment, both CrbZIP1u and CrbZIP1s proteins were detectable in the protein preparations from both CC-4533 and C-9 cells (Figure 1E, Supplemental Figure 2A). In addition to tunicamycin, treatment with another ER stress agent, dithiothreitol (DTT), also induced both CrbZIP1u and CrbZIP1s proteins in the CC-4533 and C-9 cells (Figure 1E, Supplemental

Figure 2A). However, in the *crire1* mutants, only a CrbZIP1u protein band, but not a CrbZIP1s protein band, was detected (Figure 1E, Supplemental Figure 2A). Thus, the *CrbZIP1* spliced under ER stress might be the downstream target mRNA of CrIRE1.

CrbZIP1 protein levels increased under the ER stress conditions imposed by both tunicamycin and DTT (Figure 1E, Supplemental Figure 2A); the CrbZIP1u protein level, which was very low or absent under normal conditions (0 h in Figure 1E and Supplemental Figure 2A), increased after treatment with the ER stress inducers (2 and 6 h in Figure 1E and Supplemental Figure 2A). This rapid and large induction of CrbZIP1 proteins was in contrast to the stable level of *CrbZIP1u* transcript (Figure 1B) and suggested that ER stress induces the translation of CrbZIP1u protein. Similar regulation of translation was reported in animal cells; the translation of the *XBP1u* mRNA, the target mRNA of human IRE1, is paused at the N terminus of XBP1 under normal conditions but resumes rapidly under ER stress (Yanagitani et al., 2009; Yanagitani et al., 2011).

Spliced CrbZIP1s is translocated to the nucleus from the ER

Next, to test whether the splicing of *CrbZIP1u* mRNA, which was predicted to remove the transmembrane domain, altered the subcellular localization of CrbZIP1s protein, we transiently expressed CrbZIP1 proteins fused with superfolder GFP (sGFP) at their C-termini in *Nicotiana benthamiana* epidermal cells. CrbZIP1u-sGFP colocalized with the ER marker AtBiP1-tagRFP, whereas CrbZIP1s-sGFP colocalized with the nucleus marker DAPI (Figure 1F). Together, these results suggest that ER stress activates the RNase activity of CrIRE1, which splices *CrbZIP1u* transcript to *CrbZIP1s*, and the resulting CrbZIP1s localizes to the nucleus, consistent with its function as a transcription factor.

***crbzip1* mutants are hypersensitive to ER stress**

To characterize the function of *CrbZIP1* in *Chlamydomonas*, we used two independent lines of *crbzip1* mutants: *crbzip1-1,* which was isolated from mutant pools of *Chlamydomonas* strain C-9, and *crbzip1-2,* which was obtained from the Chlamydomonas mutant library (https://www.chlamylibrary.org), derived from the CC-4533 parental line. The *APHVIII* cassette, for selection on paromomycin, was inserted into the first exon of *CrbZIP1* in both mutants (Figure 2A). Immunoblot analysis showed that *crbzip1-1* and *crbzip1-2* did not contain a detectable level of CrbZIP1 proteins, indicating that both are *crbzip1* knockout mutants (Supplemental Figure 3B). We also generated complementation lines for the *crbzip1-1* and *crbzip1-2* mutants, named *crbzip1-1C* and *crbzip1-2C*, respectively, by

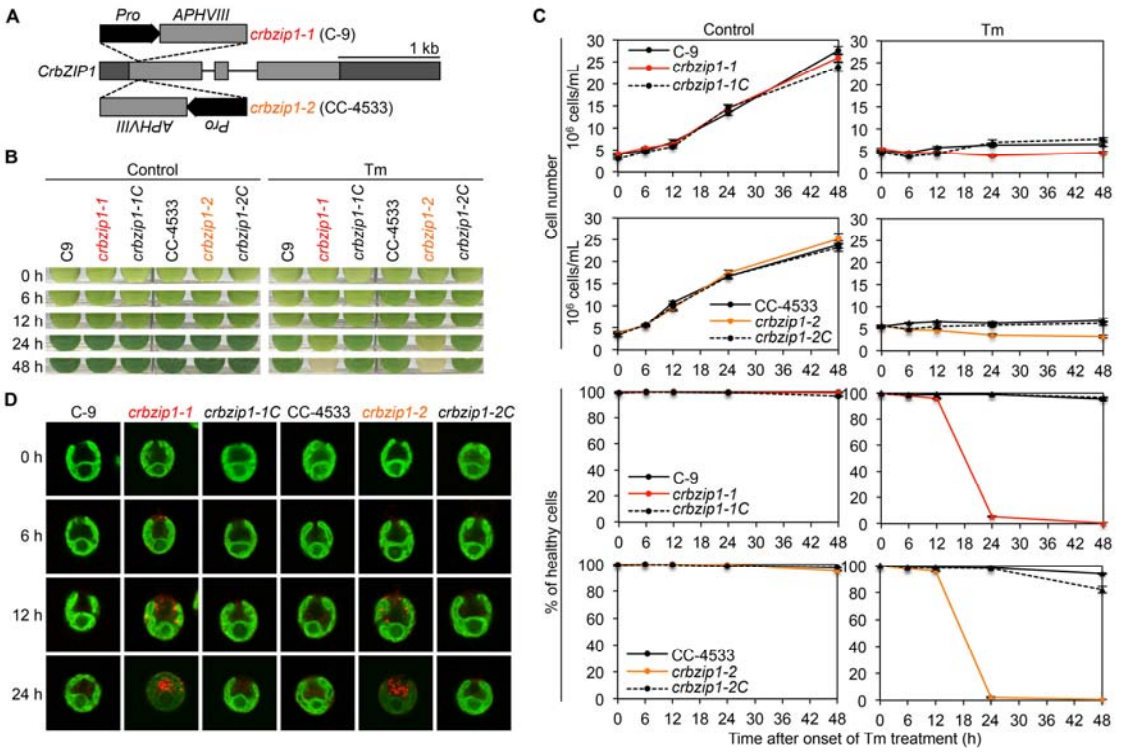

Figure 2. Isolation and phenotypic analysis of *Chlamydomonas crbzip1* mutants.
(**A**) Schematic representation of the *APHVIII* cassettes inserted into the first exon of *CrbZIP1* in the *crbzip1* mutants. The positions of UTRs, exons, and introns are indicated by dark-gray boxes, gray boxes, and lines, respectively.
(**B**) Photographs of cultures grown in control TAP medium or TAP medium containing 1 μg/mL Tm for the indicated periods.
(**C**) Cell numbers and viability of cells grown in the presence or absence of Tm. Propidium iodide (PI) was used to stain dead and damaged cells, and cells not stained with PI were considered healthy. Averages from four biological replicates from two individual experiments and their standard errors are shown.
(**D**) Confocal microscopy images of Nile red-stained cells grown in medium with 1 μg/mL Tm for 0, 6, 12, or 24 h. Images of chlorophyll autofluorescence were merged with those of Nile red fluorescence, which indicated lipid droplets.

introducing *CrbZIP1* genomic DNA into each mutant background and confirmed that the complementation lines expressed *CrbZIP1s* transcript and produced CrbZIP1 proteins (Supplemental Figure 3).

In the absence of tunicamycin, there was no difference in growth among *crbzip1-1*, *crbzip1-2*, their parental strains, and the complementation lines (Control in Figures 2B and 2C). However, after 48 h of treatment with 1 μg/mL tunicamycin, the two *crbzip1* knockout lines exhibited severe chlorosis, while their parental strains maintained green color (Figure 2B). Under ER stress conditions, growth was restored in the complementation lines to the level of the parental lines (Figures 2B and 2C), indicating that the mutations in *CrbZIP1* in the *crbzip1* mutants were responsible for their tunicamycin-sensitive phenotype. Whereas the cell numbers of the parental strains and complemented strains were slightly increased after 48 h of tunicamycin treatment, those of the *crbzip1* mutants were unchanged (Figure 2C). However, at 24 h of treatment, almost all *crbzip1* mutant cells were stained by propidium iodide, a dye that permeates dead or damaged cells (Figure 2C), suggesting serious damage

194 or death of the cells.

195 Next, we observed the lipid droplets inside the cells using the lipid-specific fluorescent
196 dye, Nile red. *crbzip1* mutants accumulated lipid droplets under ER stress, although parental
197 strains and complemented strains barely displayed the Nile red fluorescence (Figure 2D). The
198 lipid droplets in *crbzip1* mutants seemed to be present in extraplastidic regions (Figure 2D).
199
200 **CrbZIP1 is necessary for the expression of UPR genes under ER stress**
201 If CrbZIP1 has important functions in the ER stress response, the *crbzip1* mutants might
202 differ from their parental lines in the activation of genes that confer ER stress resistance.
203 Indeed, under tunicamycin treatment, the expression of genes encoding the chaperones BiP1
204 and CAL2, membrane-trafficking protein SAR1, translocon SEC61G, and disulfide forming
205 proteins ERO1, PDI6, and Pb60/PDI1A, which were reported to be involved in the ER stress
206 response (Perez-Martin et al., 2014), was upregulated only in the parental lines, and not in the
207 *crbzip1* mutants (Figure 3).

208 Interestingly, we found that the fold induction of expression by ER stress of
209 *CrbZIP1s* and many UPR genes (*CAL2*, *SAR1*, *SEC61G*, *ERO1*, and *PDI6*) was higher in
210 CC-4533 than in C-9 cells (Figure 3, Supplemental Figure 3A). This was because the
211 expression levels of these genes were lower in CC-4533 cells than in C-9 cells at the 0-h time
212 point (Supplemental Table 1). The difference in basal expression level of the
213 ER-stress-related genes might be due to the large variations in genome sequences among
214 individual *Chlamydomonas* strains (Siaut et al., 2011; Gallaher et al., 2015).
215
216 **Lipid remodeling is altered in the *crbzip1* mutants upon ER stress**
217 Lipid remodeling is known to be essential for cell survival under cold stress (Moellering et al.,
218 2010), but it is not clear if it also plays a role in the cell's response to ER stress. To
219 investigate the mechanisms underlying ER stress management, we analyzed the entire
220 glycerolipid profiles of the *crbzip1* mutants and their parental strains under ER stress. After
221 tunicamycin treatment, the mol% of TAG content did not increase very much from the
222 starting value (0 h) in the parental lines; however, this value dramatically increased in the
223 *crbzip1-1* and *crbzip1-2* mutants and was 5.8- and 9.4-fold that of each parental strain,
224 respectively (Figure 4A, red boxes). Consistent with this result, the expression level of the
225 gene encoding a key enzyme involved in TAG biosynthesis, ER-type DGTT1, was
226 up-regulated only in the *crbzip1* mutants after tunicamycin treatment (Figures 4B and 4C),
227 but the expression of genes encoding other acyltransferases was not up-regulated in the

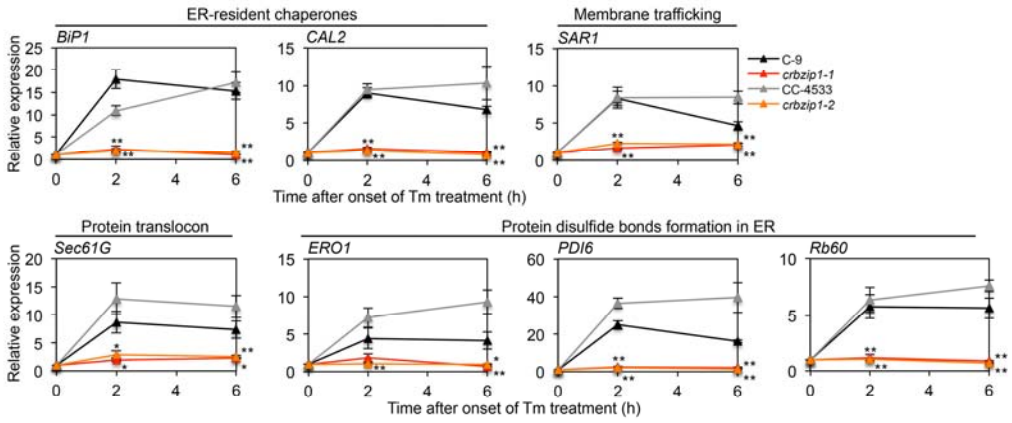

Figure 3. Expression levels of ER stress marker genes in *crbzip1* mutants and their parental strains.
Cells were treated with 1 μg/mL tunicamycin (Tm) for the indicated periods. The RT-qPCR results were normalized by the level of *RPL17* expression and the fold changes of expression levels at 2 h and 6 h were determined relative to the levels at 0 h. Error bars represent standard errors based on four biological replicates from two individual experiments. Statistical analysis was carried out using a Student's *t*-test (*, $p < 0.05$; **, $p < 0.01$) and the Wilcoxon rank sum test (Supplemental Dataset 1).

crbzip1 mutants (Supplemental Figure 4).

To determine the source of the fatty acids used for TAG biosynthesis in the *crbzip1* mutants, we compared the major glycerolipid content of *crbzip1* cells with that of their parental lines. After 12 h of treatment, the most striking difference was the mol% of a major extraplastidic membrane lipid, DGTS (Giroud et al., 1988), which decreased in *crbzip1* mutants, but increased in parental lines (Figure 4A, green boxes). This result suggests that the fatty acids in the TAGs formed in *crbzip1* cells during ER stress were derived from ER membrane lipid. To determine how DGTS levels increased in the parental lines, we assayed the expression level of *BTA1*, which encodes a key enzyme in DGTS biosynthesis in *Chlamydomonas* (Riekhof et al., 2005). *BTA1* expression increased under ER stress, in the parental lines and complementation lines, but not in the *crbzip1* mutants (Figures 4D and 4E, Supplemental Figure 5). Furthermore, CrbZIP1s protein directly bound to the promoter region of *BTA1* in a yeast one-hybrid assay (Figure 4F). These results suggest that CrbZIP1s up-regulates *BTA1* expression and thus the production of DGTS synthesis under ER stress in *Chlamydomonas*.

CrbZIP1 expression is necessary for ER stress-induced biosynthesis of pinolenic acid, which enhances ER stress tolerance

Next, we analyzed the fatty acid composition of the *crbzip1* mutants and their parental strains. During ER stress, the abundance of pinolenic acid (18:3Δ5,9,12) and coniferonic acid (18:4Δ5,9,12,15) in the total fatty acids was increased in the parental strains but was reduced in the *crbzip1* mutants (Figure 4A, blue boxes). Subsequent analysis of fatty acid composition of individual glycerolipids revealed that the pinolenic acid content in DGTS differed

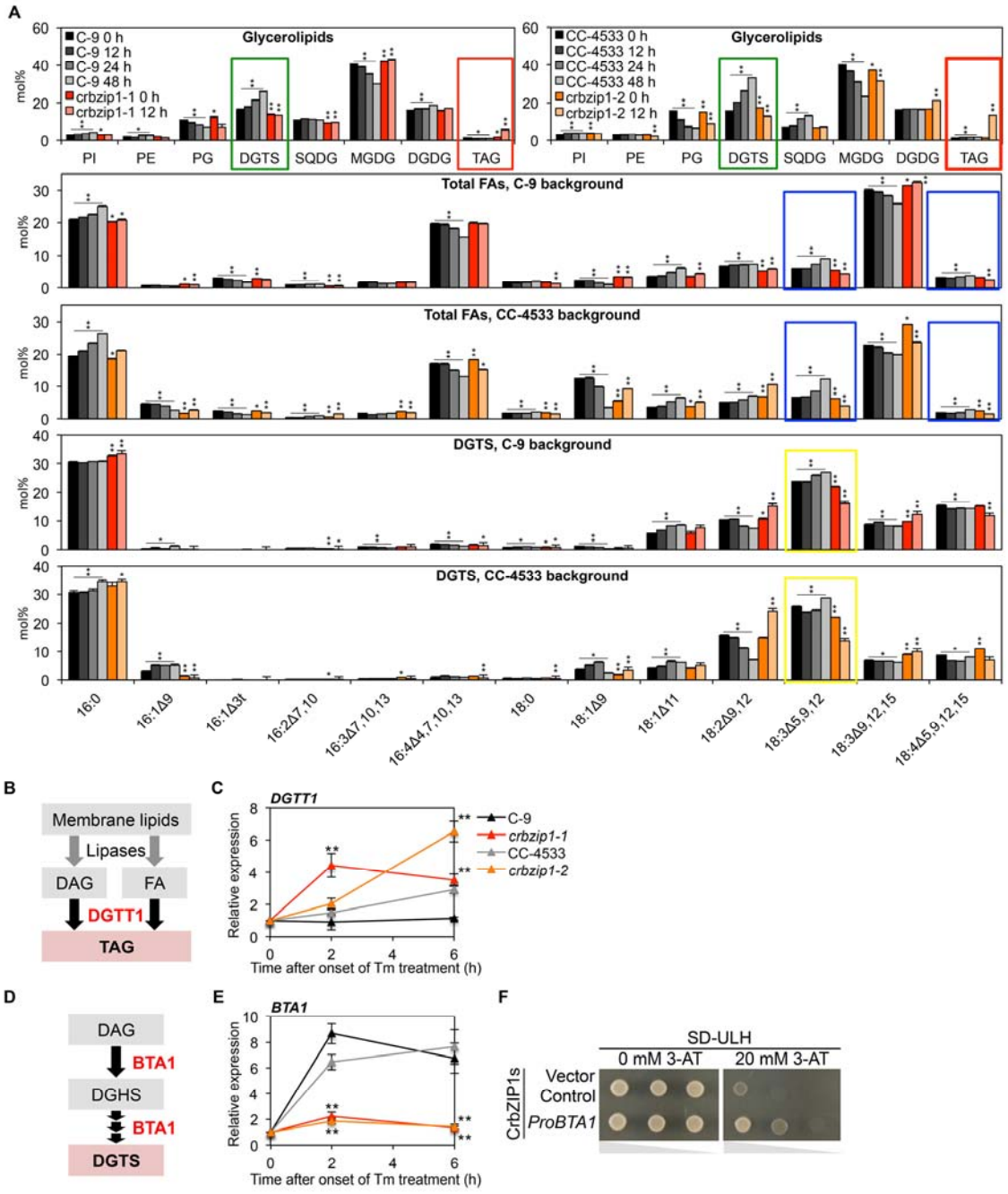

Figure 4. ER-stress-induced lipid remodeling differs between the *crbzip1* mutant and their parental lines.

dramatically between the *crbzip1* mutants and their parental lines (Figure 4A, Supplemental Figure 6). In DGTS, the pinolenic acid content slightly increased in parental strains but decreased greatly in the *crbzip1* mutants after tunicamycin treatment (Figure 4A, yellow boxes). Pinolenic acid biosynthesis in the ER requires the desaturases FAD2 and CrDES in *Chlamydomonas* (Kajikawa et al., 2006). *FAD2* and *CrDES* expression increased significantly in the parental strains, but not in the *crbzip1* mutants, upon treatment with tunicamycin (Figure 5B), suggesting that CrbZIP1 induces these desaturases. This possibility

Figure 4. ER-stress-induced lipid remodeling differs between the *crbzip1* mutant and their parental lines.
(**A**) Levels of fatty acids (FAs) in glycerolipids and the fatty acid composition of total fatty acids and of diacylglyceryltrimethylhomo-Ser (DGTS). Lipids extracted from *crbzip1* mutants and their parental strains treated with 1 μg/mL tunicamycin (Tm) for the indicated periods were analyzed using GC-FID. Error bars represent standard errors based on three biological replicates. Red box indicates TAG accumulation in *crbzip1* cells. Green box represents the induction of DGTS only in the parental strains. Blue boxes indicate the decreases of pinolenic acid in total FAs in *crbzip1* cells. Yellow boxes indicate the dramatic reductions of pinolenic acid in DGTS. phosphatidylinositol (PI), phosphatidylethanolamine (PE), phosphatidylglycerol (PG), sulfoquinovosyldiacylglycerol (SQDG), monogalactosyldiacylglycerol (MGDG), digalactosyldiacylglycerol (DGDG), and triacylglycerol (TAG). Statistical analysis was carried out using a Student's *t*-test (*, $p < 0.05$; **, $p < 0.01$, Supplemental Dataset 2), and the significant differences between the mutant and the parental strain at the same time point are marked.
(**B**) Major TAG biosynthesis pathway mediated by DGTT1 in *Chlamydomonas*. DGTT1 is a critical enzyme for TAG synthesis in *Chlamydomonas*.
(**C**) Expression levels of *DGTT1* under ER stress. Cells were treated with 1 μg/mL Tm for the indicated periods. The RT-qPCR results were normalized by the level of *RPL17* expression and the fold changes of expression levels were determined relative to the levels at 0 h. Error bars represent standard errors based on four biological replicates at 0, 2, and 6 h. Statistical analysis was carried out using a Student's *t*-test (**, $p < 0.01$) and the Wilcoxon rank sum test (Supplemental Dataset 1).
(**D**) DGTS biosynthesis pathway mediated by BTA1 in *Chlamydomonas*. BTA1 is a critical enzyme for DGTS biosynthesis in *Chlamydomonas*.
(**E**) Expression level of *BTA1* in *Chlamydomonas* cells subjected to ER stress. Experimental conditions and data processing were the same as in (C).
(**F**) Yeast one-hybrid assay showing that CrbZIP1s interacts directly with the promoter region of *BTA1*. Yeast cells were spotted on medium containing SD-Leu-Ura-His with or without 3-AT with a series of 1:10 dilutions.

was supported by a yeast one-hybrid assay, which revealed that CrbZIP1s interacted directly with the promoter region of *CrDES* (Figure 5C). By contrast, the *FAD7* transcript level was induced both in the parental lines and in the *crbzip1* mutants (Figure 5B), indicating that the production of alpha-linolenic acid (18:3Δ9,12,15) or coniferonic acid (18:4Δ5,9,12,15) is not the downstream target of CrbZIP1.

We then hypothesized that the induction of pinolenic acid in *Chlamydomonas* cells might protect the cells from ER stress. To address this possibility, we isolated *crdes1-1* and *crdes1-2* mutants in the C-9 and CC-4533 background, respectively (Figure 6A, Supplemental Figure 7). The *crdes1-1* mutant did not contain detectable amounts of pinolenic acid (18:3Δ5,9,12) or coniferonic acid (18:4 Δ5,9,12,15; Figure 6B, blue arrows in Total FAs), and the *crdes1-2* mutant contained lower levels of the two compounds than the parental line (Figure 6B, green arrows in Total FAs, yellow boxes in DGTS; Supplemental Figure 8, yellow boxes in PE and TAG), suggesting that *crdes1-1* is a knockout mutant and *crdes1-2* is a knockdown mutant. The fatty acid composition of other major glycerolipid species was not altered much in the *crdes* mutants (Supplemental Figure 8). Although the pinolenic acid content of PE and DGTS was reduced relative to the parental lines, the DGTS and PE contents were maintained in the *crdes* mutants (Figure 6B, Glycerolipids). The increase in alpha-linolenic acid (18:3Δ9,12,15) appeared to compensate for the loss of pinolenic acid in PE and DGTS in both the *crdes* mutants (Figures 6B, Supplemental Figure 8, red boxes).

Next, we investigated whether the two *crdes* mutants differed from their parental lines with respect to ER stress resistance. No difference in growth between any of the *Chlamydomonas* strains was apparent when the cells were cultured on normal TAP medium (Figure 6C, TAP). However, when the strains were spotted on TAP medium containing 0.2

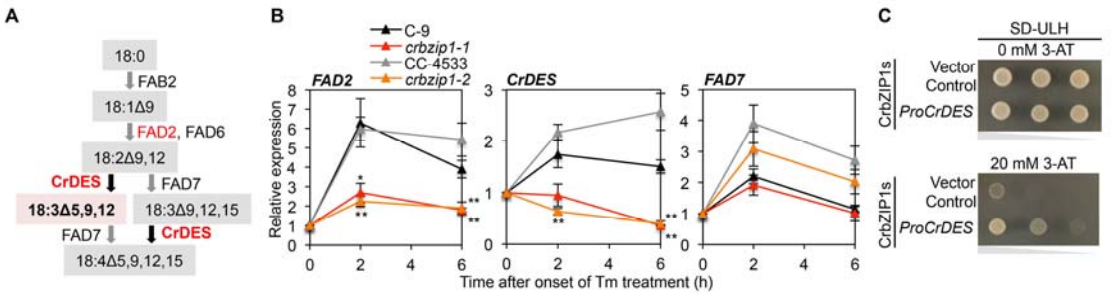

Figure 5. CrbZIP1s promotes the biosynthesis of pinolenic acid (18:3Δ5,9,12) under ER stress.
(**A**) C18 FA biosynthesis pathway in *Chlamydomonas*.
(**B**) Relative transcript abundance of desaturase genes after tunicamycin (Tm) treatment. Cells were treated with 1 μg/mL Tm for the indicated periods. The RT-qPCR results were normalized by the level of *RPL17* expression and the fold changes of expression levels were determined relative to the levels at 0 h. Error bars represent standard errors based on four biological replicates for 0, 2, and 6 h. Statistical analysis was carried out using a Student's *t*-test (*, $p < 0.05$; **, $p < 0.01$) and the Wilcoxon rank sum test (Supplemental Dataset 1).
(**C**) Yeast one-hybrid assay showing that CrbZIP1s interacts directly with the promoter region of *CrDES*. Yeast cells were spotted on medium containing SD-Leu-Ura-His with or without 3-AT with a series of 1:10 dilutions.

μg/mL tunicamycin, *crdes* mutants exhibited hypersensitivity to ER stress, similarly to *crbzip1* mutants (Figure 6C, TAP + Tm). These data suggest that CrbZIP1-mediated pinolenic acid biosynthesis improves the survival of *Chlamydomonas* exposed to ER stress.

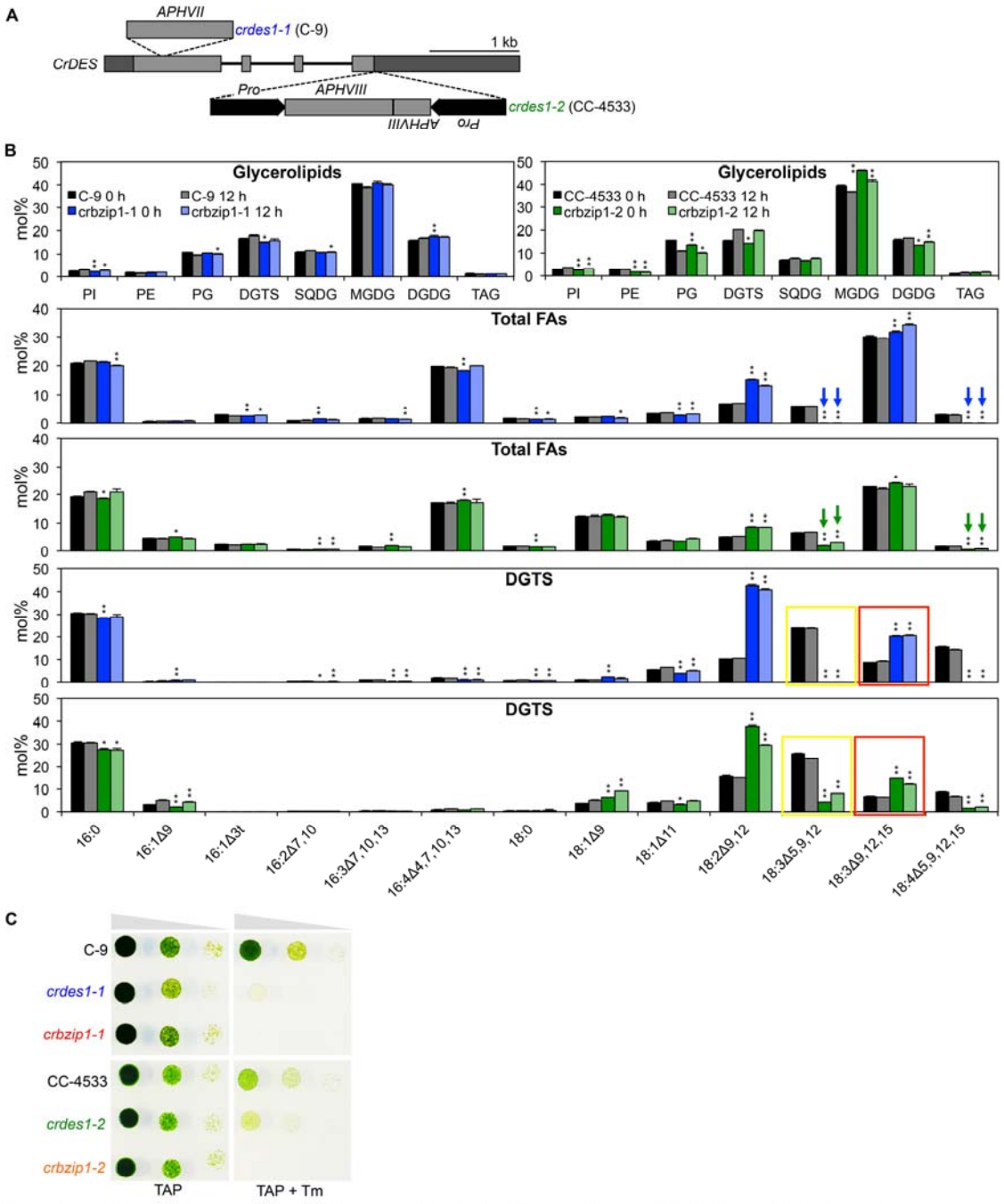

Figure 6. *crdes* knockdown mutants are hypersensitive to the ER stress imposed by tunicamycin treatment.

DISCUSSION

CrbZIP1 functions downstream of CrIRE1 and plays a critical role in the ER stress response

In microalgae, no transcription factor has been identified that functions downstream of the ER stress sensor. In this study, we established that the *Chlamydomonas* transcription factor CrbZIP1 functions downstream of CrIRE1, and activates the expression of many genes that

Figure 6. *crdes* knockdown mutants are hypersensitive to the ER stress imposed by tunicamycin treatment.
(**A**) Schematic representation of insertion sites of the *APHVII* and *APHVIII* cassettes in the genomic sequence of *CrDES* in *crdes* mutants. The positions of UTRs, exons, and introns are indicated by dark-gray boxes, gray boxes, and lines, respectively.
(**B**) Levels of fatty acids (FAs) in glycerolipids and fatty acid composition of total fatty acids, phosphatidylethanolamine (PE), and diacylglyceryltrimethylhomo-Ser (DGTS). Total lipids were extracted from cells treated with 1 μg/mL tunicamycin (Tm) for the indicated periods. Blue arrows and green arrows indicate absence or reduction of pinolenic acid and coniferonic acid in *crdes1-1* and *crdes1-2* mutants, respectively. Yellow boxes indicate absence or reduction of pinolenic acid in *crdes1-1* or *crdes1-2* mutants, respectively. Red boxes indicate compensatory increases of alpha-linolenic acid in *crdes1* mutants. Error bars represent standard errors based on three biological replicates. Statistical analysis was performed as described in Supplemental Dataset 3.
(**C**) Growth of the indicated *Chlamydomonas* cell lines spotted on TAP medium supplemented with or without 0.2 μg/mL Tm with a series of 1:10 dilutions.

contribute to survival under ER stress. The following observations support this conclusion. First, *CrbZIP1* mRNA was spliced under ER stress in *Chlamydomonas* cells, but this splicing activity was very low in *crire1* knockdown mutants (Figure 1B). Second, two independent mutant alleles of CrbZIP1, *crbzip1-1* and *crbzip1-2*, which did not exhibit any growth defect under normal conditions, exhibited increased sensitivity to ER stress: they were completely bleached within 2 days of exposure to a concentration of tunicamycin that did not induce chlorosis in their parental lines (Figure 2B). Third, CrbZIP1 upregulated the expression of ER stress response genes, including chaperone genes and lipid biosynthesis genes (Figure 3). We also obtained data that are consistent with CrbZIP1 having a role in the ER stress response: CrbZIP1 levels increased under ER stress (Figure 1E), and the CrbZIP1s protein encoded by the spliced form of *CrbZIP1* was localized in the nucleus (Figure 1F).

Increase in pinolenic acid content protects the cells during ER stress

Pinolenic acid levels increased in the parental strains, but dramatically decreased in the *crbzip1* mutants under ER stress (Figure 4A). Pinolenic acid (18:3Δ5,9,12), a Δ5-desaturated metabolite of linoleic acid (18:2Δ9,12), is found in the oil of Korean pine (*Pinus koraiensis*) nuts and needles and in some microalgae. A polymethylene group within the carbon skeleton of pinolenic acid makes it structurally distinct from its positional isomer gamma-linolenic acid (18:3Δ6,9,12). Pinolenic acid was demonstrated to provide specific health benefits not imparted by several other 18:3 fatty acid species (Asset et al., 2000; Asset et al., 2001; Lee et al., 2004; Pasman et al 2008). *Chlamydomonas* was reported to produce pinolenic acid, but the physiological role of this fatty acid in this alga remained unknown (Giroud et al., 1988). In this study, we isolated two independent mutants of *CrDES*, a desaturase required for pinolenic acid production, and found that the *crdes* mutants were much more impaired in growth in medium containing tunicamycin than were their parental lines (Figure 6C). Notably, the *crdes1-1* knockout mutant displayed ER stress hypersensitivity comparable to that of the *crbzip1-1* mutant (Figure 6C), suggesting that the upregulation of *CrDES* is one of the major routes through which CrbZIP1 confers ER stress resistance in *Chlamydomonas*. Furthermore,

the yeast one-hybrid assay suggested that CrbZIP1s directly regulates *CrDES* expression (Figure 5C). Therefore, CrbZIP1-dependent pinolenic acid biosynthesis seems to be necessary for effective protection of this microalga from ER stress. Since pinolenic acid is produced only in a limited number of organisms, these results also indicate that ER stress tolerance mechanisms differ among various organisms.

How does pinolenic acid enhance tolerance to ER stress in *Chlamydomonas*? Previous reports revealed that reactive oxygen species (ROS) are induced by ER stress in *Chlamydomonas* cells (Pérez-Martín et al., 2014), and that polyunsaturated fatty acids in membrane lipids act as sinks for ROS in plastids (Mene-Saffrane et al., 2009; Zeoeller et al., 2012). Thus, pinolenic acid might be able to mitigate ROS toxicity. However, this general effect of polyunsaturated fatty acids does not explain the effect of pinolenic acid in ER stress resistance in *Chlamydomonas*, since the levels of another polyunsaturated fatty acid, alpha-linolenic acid (18:3Δ6,9,12), increased in DGTS and PE in *crdes* mutants (Figure 6B, Supplemental Figure 8), but failed to protect the cells from ER stress (Figure 6C). Another possibility is that pinolenic acid functions as a signaling molecule, much like jasmonic acid in many terrestrial plants. Trees in the Pinus family (Pinaceae) are among the longest living plants on Earth (Rogers and Clifford, 2006; Withington et al., 2006). Thus, it is tempting to speculate that pinolenic acid in the leaves of these trees confers ER stress resistance and consequently contributes to the longevity of the plant. Further studies are needed to understand the protective function of pinolenic acid in *Chlamydomonas* subjected to ER stress, and it would be interesting to test whether pinolenic acid confers ER stress resistance in other organisms, too.

Increase of DGTS under ER stress

Some algae, including *Chlamydomonas,* have been reported to contain DGTS but not phosphatidylcholine (PC) in the ER membrane (Kato et al., 1996). Our study revealed that CrbZIP1 directly upregulated the expression of the DGTS synthase gene *BTA1*, and that DGTS content significantly increased in the parental lines but not in the *crbzip1* mutants under ER stress (Figure 4A, Glycerolipids). An increase in ER membrane lipids was also observed in other organisms exposed to ER stress. In animals, XBP1 plays an important role in the biosynthesis of PC, the main ER phospholipid, which allows ER membrane expansion under ER stress (Sriburi et al., 2007). Furthermore, in yeast, the increase in ER size by upregulation of PC biosynthesis improves ER stress tolerance (Schuck et al., 2009). By analogy with these studies in animals and yeast, we hypothesized that the increase in DGTS

levels in *Chlamydomonas* cells might contribute to their survival under ER stress by expanding the ER membrane. In DGTS, the polar betaine trimethylglycine is linked by an ether bond at the *sn*-3 position of the glycerol moiety. Trimethylglycine is an osmolyte that stabilizes proteins under many stress conditions (Auton et al., 2011). Covering the surface of the ER lumen with trimethylglycine might mediate protein folding under ER stress in *Chlamydomonas*. Thus, it would be interesting to study the biological function of this betaine lipid further.

***crbzip1* mutations induce hypersensitivity to ER stress and promote the formation of lipid droplets**

crbzip1 mutants accumulated lipid droplets under the ER stress induced by tunicamycin (Figure 2D). Lipid droplets were also observed in *crire1* mutants treated with the same concentration (1 μg/mL) of tunicamycin (Yamaoka et al., 2018). These results imply that mutations in the CrIRE1/CrbZIP1 pathway disrupt the regular UPR under ER stress, resulting in the accumulation of lipid droplets and rendering these mutants more vulnerable to stress than their parental lines. The biosynthesis of the lipids accumulated in the lipid droplets seemed to be catalyzed by an acyltransferase, *DGTT1*, previously shown to play a major role in TAG accumulation under nitrogen starvation stress (Boyle et al., 2012), since the gene encoding this protein was expressed at higher levels in *crbzip1* mutants than in their parental strains under ER stress (Figure 4C).

In summary, we established CrbZIP1 as the target of CrIRE1 under ER stress, and provided insight into the CrIRE1/CrbZIP1-mediated response to ER stress in *Chlamydomonas* (Figure 7). Under the ER stress induced by 1 μg/mL tunicamycin, *CrbZIP1* is activated by cleavage and upregulates the expression of general UPR genes and of genes encoding DGTS synthase and pinolenic acid synthase, and thereby overcomes the stress. However, in the absence of functional CrIRE1/CrbZIP1 proteins, *Chlamydomonas* cells exhibited another stress response strategy and stress symptom, namely the induction of acyltransferase and the formation of lipid droplets. Our data clearly indicate that lipid modifications contribute to the survival of the *Chlamydomonas* cells exposed to ER stress. It would be very interesting to test whether similar lipid modifications occur during the ER stress response in other organisms. We predict that some aspects of the lipid modification revealed here might be common to the ER stress response in many organisms, since the IRE1-mediated ER stress response pathway is highly conserved (Howell 2013; Ron and Walter 2007; Yamaoka et al., 2018).

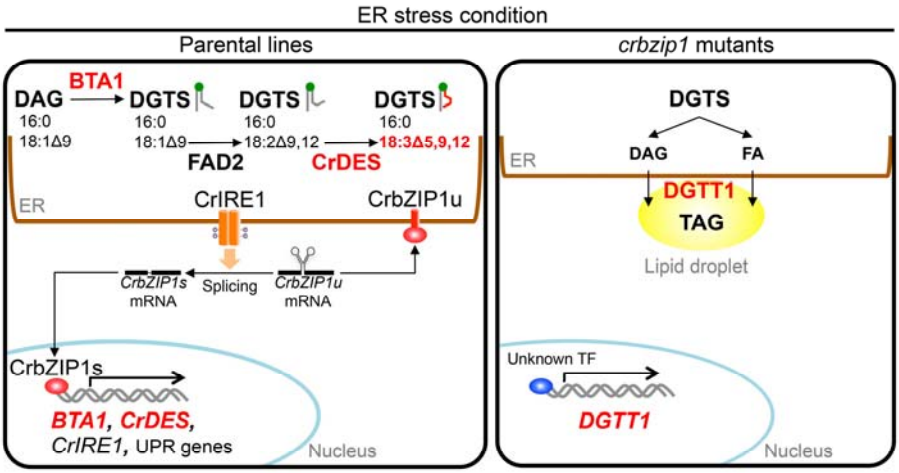

Figure 7. Proposed model for a mechanism of ER stress responses in *crbzip1* mutants and their parental lines in *Chlamydomonas*.
Left: In the parental lines, activated CrIRE1 splices C*rbZIP1u* mRNA to produce *CrbZIP1s,* which is translated to CrbZIP1s. CrbZIP1s enters the nucleus, where it induces the expression of UPR genes and ER membrane lipid biosynthesis genes, such as *BTA1* and *CrDES*. The dimerization and phosphorylation of CrIRE1 are drawn based on reports in other organisms but have not been revealed in *Chlamydomonas.*
Right: The *crbzip1* mutation upregulates TAG biosynthesis from the fatty acids hydrolyzed from a major ER membrane lipid, DGTS, resulting in the formation of lipid droplets, which store TAGs.

388

389

METHODS

Strains and culture conditions

The *Chlamydomonas* strain C-9 (CC-5098, *mt*$^-$), originally provided by the IAM Culture Collection at The University of Tokyo and available from the Chlamydomonas Resource Center, was used as the parental strain. The *crbzip1-1* and *crdes1-1* mutants, containing the *APHVIII* and *APHVII* insertions, respectively, were isolated in accordance with a previous report (Yamano et al., 2015). The *Chlamydomonas* strain CC-4533 (*cw15 mt*$^-$) and the *crbzip1-2* (LMJ.RY0402.143080) and *credes1-2* (LMJ.RY0402.087433) mutants were obtained from the Chlamydomonas Genetics Center (USA) (Li et al., 2016). *Chlamydomonas* cells were cultured in an Erlenmeyer flask containing Tris-acetate-phosphate (TAP) medium (Harris, 2009) at 23°C under continuous light (75 μmol photons m^{-2} s^{-1}) supplied by tubular fluorescent lamps (color temperature 4000K) with shaking at 190 rpm. Cells in the exponential growth phase ($3x10^6$ cells/mL) were treated with the indicated concentration of tunicamycin (Sigma-Aldrich, T7765) diluted from a 5 mg/mL stock in 0.05 N NaOH or DTT (dithiothreitol; Duchefa Biochemie, Netherlands) diluted from a 1 M stock in water. Dead cells were stained with 2 μg/mL propidium iodide for 15 min in darkness, as described in Kim et al. (2015), and cells immobilized in 1% (w/v) low-gelling agarose (Sigma-Aldrich) were counted using a hemocytometer under a fluorescence microscope (Nikon Optiphot microscope) with a TRITC filter.

Phylogenetic tree analyses

Amino acid sequences were obtained from Phytozome v12.1 (https://phytozome.jgi.doe.gov), TAIR (https://www.arabidopsis.org), and the *Saccharomyces* Genome Database (http://www.yeastgenome.org) and were aligned using the Clustal Omega algorithm (Sievers et al., 2011). The phylogenetic tree was constructed using MEGA 7.0 (Kumar et al., 2016) with 1,000 bootstrap replicates.

Immunoblot analysis

Anti-CrbZIP1 antibody was generated against a synthetic peptide containing the 23-amino acid fragment located at the N-terminus of CrbZIP1 (GPSLLDDELFSEDLMQFLETIEG). Rabbits were injected with the peptide for the production of anti-CrbZIP1 polyclonal antibody (Young In Frontier, South Korea). To detect CrbZIP1 protein levels, total protein was extracted from *Chlamydomonas* cells and 40 μg of total protein was subjected to immunoblot analysis as described previously (Song et al., 2004).

Subcellular localization of CrbZIP1 in *Nicotiana benthamiana* epidermal cells

CrbZIP1u and *CrbZIP1s* cDNA were introduced into pGWB5 (Nakagawa et al., 2007). *Arabidopsis* BiP1 cDNA were introduced into pGWB560 (Nakagawa et al., 2008). *N. benthamiana* leaves were infiltrated as described previously (Sparkes et al., 2006).

Microscopy analysis

To visualize lipid droplets, cells were stained with 1 μg/mL Nile red (Sigma-Aldrich) diluted from a 0.1 mg/mL stock solution in acetone for 20 min in darkness at room temperature, and the cells were immobilized in 1% (w/v) low-gelling agarose (Sigma-Aldrich). To visualize the nucleus, the DAPI staining was performed as described by Yamaoka et al. (2011). Fluorescence was observed using a confocal laser-scanning microscope (Olympus).

RNA extraction and quantification

Total RNA was extracted and quantified as described previously (Jang et al., 2015), with a few modifications. Total RNA was isolated using homemade TRIzol, and cDNA was synthesized using a RevertAid First Strand cDNA Synthesis Kit (K1621, Thermo Scientific) and 3 μg of total RNA. Quantitative RT-PCR was performed using SYBR Premix Ex Taq (Takara) and the primer sets are listed in Supplemental Table 1. The quantitative RT-PCR results were normalized by the level of *RPL17* expression (Yamaoka et al., 2018).

Isolation of complementation strains

The promoter region of the *Chlamydomonas* expression vector pChlamy_1 (Thermo Scientific) was removed, and the *CrbZIP1* promoter region fused with the 5′-UTR (2135 bp) and the CrbZIP1 genomic DNA with the 3′-UTR (2911 bp) was inserted as a *Xba*I fragment (pChlamy-CrbZIP1). *crbizp1-1* and *crbzip1-2* were transformed with pChlamy-CrbZIP1, and the transformants were selected by hygromycin tolerance. CrbZIP1 proteins from 96 transformants were individually analyzed by immunoblot assay, and the transformants that contained similar amounts of CrbZIP1 proteins to the parental strains were selected as complementation lines of *crbzip1* mutants.

Lipid extraction and quantification

Lipids were extracted and analyzed as described previously (Kim et al., 2013) with

modifications. Briefly, 40 mL of *Chlamydomonas* cell culture (approximately 5 x 10^6 cells/mL) was harvested by centrifugation at 2,000 *g* for 5 min at room temperature and used for total lipid extraction. To quantify TAGs, 1 mg of the total lipid extract was separated on a thin-layer chromatography (TLC) plate using the following solvent mixture: hexane:diethyl ether:acetic acid (80:30:1, by volume). To separate membrane lipids, 1 mg of the total lipid extract was separated on a TLC plate using the following solvent mixture: chloroform:methanol:acetic acid:water (75:13:9:3, by volume). Lipid spots were visualized under UV after spraying with 0.01% (w/v) primuline (Sigma) dissolved in acetone:H_2O (4:1, v/v). Lipid bands were recovered from the plate and quantified by a gas chromatograph (GC-FID, SHIMADZU GC-2010) equipped with an HP-INNOWax capillary column (30 m × 0.25 mm, 0.25 μm film thickness, Agilent Technologies) after transesterification.

Yeast one-hybrid assay

Yeast one-hybrid assays were carried out using the Matchmaker™ Yeast One-HybridSystem (Clontech, USA), as described in the manufacturer's protocol. The promoters of *BTA1* (655 bp) and *CrDES* (736 bp) were cloned into the pHISi vector, and codon-optimized CrbZIP1s for yeast expression was subcloned into the pGAD424 vector using the primers listed in Table S1. Yeast cells were spotted on medium containing SD-Leu-Ura-His with or without 3-AT with a series of 1:10 dilutions.

Accession Numbers

Chlamydomonas genes analyzed in this study were identified in Phytozome v12 (http://phytozome.jgi.doe.gov/pz/portal.html) under the following accession numbers: *CrbZIP1*, Cre05.g238250.t1.2; *CrIRE1*, Cre08.g371052.t1.1; *BiP1*, Cre02.g080700.t1.2; *CAL2,* Cre01.g038400.t1.2; *SAR1*, Cre11.g468300.t1.2; *SEC61*, Cre16.g680230.t1.1; *ERO1*, Cre17.g723150.t1.3; *PDI6*, Cre12.g518200.t1.3; *Rb60,* Cre02.g088200.t1.2; *DGTT1;* Cre12.g557750.t1.1; *BTA1*, Cre07.g324200.t1.2; *FAD2*, Cre17.g711150.t1.1; *CrDES*, Cre10.g453600.t2.1; *FAD7*, Cre01.g038600.t1.2; *PDAT*, Cre02.g106400.t1.1; *DGAT*, Cre01.g045903.t1.1; *DGTT2*, Cre09.g386912.t1.1; *DGTT3*, Cre06.g299050.t1.2; *DGTT4*, Cre03.g205050.t1.2. Arabidopsis genes analyzed in this study were identified in TAIR (https://www.arabidopsis.org) under the following accession numbers: *AtbZIP60*, AT1G42990.1; *AtBiP1*, AT5G28540.1. The yeast gene analyzed in this study was identified in the *Saccharomyces* Genome Database (http://www.yeastgenome.org) under the following accession number: *Hac1,* S000001863.

Supplemental Data

Supplemental Figure 1. The splicing motif of *CrbZIP1* mRNA differs from that of *AtbZIP60, ScHAC1,* and *HsXBP1* mRNA.

Supplemental Figure 2. Immunoblot analysis of CrbZIP1u and CrbZIP1s.

Supplemental Figure 3. Isolation of complementation strains of *crbzip1* mutants.

Supplemental Figure 4. Expression levels of acyltransferase genes in *crbzip1* mutants and their parental strains under the ER stress.

Supplemental Figure 5. Expression levels of *BTA1* and *CrDES* were recovered in the *crbzip1-1C* and *crbzip1-2C* lines.

Supplemental Figure 6. Fatty acid compositions of glycerolipids in *crbzip1* mutants subjected to ER stress.

Supplemental Figure 7. Isolation of *Chlamydomonas crdes1-1* and *crdes1-2* mutants.

Supplemental Figure 8. Fatty acid compositions of glycerolipids in *crdes* mutants subjected to ER stress.

Supplemental Table 1. Expression levels of ER stress sensor and ER stress marker genes in *crbzip1* mutants and their parental strains.

Supplemental Table 2. Primer sequences.

Supplemental Dataset 1. Statistical analyses for transcript levels.

Supplemental Dataset 2. Statistical analyses for lipid content of *crbzip1* mutants and their parental strains.

Supplemental Dataset 3. Statistical analyses for lipid content of *crdes* mutants and their

parental strains.

ACKNOWLEDGMENTS

This work was supported by the Advanced Biomass R&D Center (ABC) of Global Frontier Project funded by the Ministry of Science, ICT and Future Planning (ABC-2015M3A6A2065746) awarded to Y. Lee, the Japan Society for the Promotion of Science KAKENHI (16H04805) and the Japan Science and Technology Agency, Advanced Low Carbon Technology Research and Development Program (ALCA, JPMJAL1105) awarded to H. Fukuzawa, Agence Nationale de la Recherche (ANR-MUsCA) awarded to Y. Li-Beisson, and the Korea Research Fellowship Program funded by the Ministry of Science, ICT and Future Planning through the National Research Foundation of Korea (2016H1D3A1909463) to Y. Yamaoka. We thank the *Chlamydomonas* Mutant Library Group at the Carnegie Institution for Science and the *Chlamydomonas* Resource Center at the University of Minnesota for providing the indexed *Chlamydomonas* insertional mutants.

AUTHOR CONTRIBUTIONS

Y.Y., Y.L.-B., and Y.L. contributed to design of the research. Y.Y., S.S., B.Y.C., H.K., and S.J. performed the research. T.Y. and H.F. produced mutant library using *Chlamydomonas* strain C-9. Y.Y. and S.S. isolated *crbzip1-1* mutant, and M.K. isolated *crdes1-1* mutant. Y.Y., F.K., B.L., and Y.L.-B. performed lipid analysis. Y.Y., Y.L.-B., and Y.L. wrote and revised the manuscript.

SUPPLEMENTAL DATA

Supplemental Figure 1. The splicing motif of *CrbZIP1* mRNA differs from that of *AtbZIP60, ScHAC1,* and *HsXBP1* mRNA. Supports Figure 1C.

Stem-loop structures predicted for the mRNAs of *CrbZIP1, AtbZIP60*, *ScHAC1,* and *HsXBP1*. The conserved nucleotides essential for splicing of *AtbZIP60, ScHAC1,* and *HsXBP1* mRNAs are enclosed in boxes. Red arrowheads indicate the splicing sites observed in target mRNAs of IRE1. The structure of *CrbZIP1* was predicted using CentroidFold. The structures of *AtbZIP60*, *ScHAC1,* and *HsXBP1* were adapted from Nagashima et al., 2011.

Supplemental Figure 2. Immunoblot analysis of CrbZIP1u and CrbZIP1s. Supports Figure 1E.

(**A**) Immunoblot analysis of CrbZIP1u (53 kDa) and CrbZIP1s (33 kDa) using anti-CrbZIP1

559 antibody. Protein preparations from cells treated with 1 μg/mL tunicamycin (Tm) or 5 mM
560 dithiothreitol (DTT) for the indicated periods were subjected to immunoblot analysis.
561 Coomassie brilliant blue staining (CBB) was used as a loading control.
562 (**B**) The size verification of CrbZIP1s expressed in *E. coli.* MBP-CrbZIPs was eluted from the
563 crude protein preparation of *E. coli* containing pMAL-c2X-CrbZIP1s using amylose resin.
564 MBP-CrbZIP1s was digested with the factor Xa, separated by SDS-PAGE, and then
565 visualized by silver staining. Although the protein size of CrbZIP1s was predicted to be 33 kDa,
566 CrbZIP1s from *Chlamydomonas* cells and recombinant CrbZIP1s protein expressed in *E. coli*
567 were found at around 25 kDa, due to some unknown reason.
568
569 **Supplemental Figure 3. Isolation of complementation strains of *crbzip1* mutants.** Supports
570 Figures 2A and 2B.
571 (**A**) Expression levels of CrbZIP1s in *crbzip1* mutants, their parental strains, and their
572 complement strains. Cells were treated with 1 μg/mL tunicamycin (Tm) for the indicated
573 periods. The RT-qPCR results were normalized by the level of *RPL17* expression, and the fold
574 changes of expression levels at 2 and 6 h were determined relative to the levels at 0 h. Error
575 bars represent standard errors based on four biological replicates from two individual
576 experiments. Statistical analysis was carried out using Student's *t*-test (*, $p < 0.05$; **, $p <$
577 0.01) and the Wilcoxon rank sum test (Supplemental Dataset 1).
578 (**B**) Immunoblot analysis of CrbZIP1 proteins using anti-CrbZIP1 antibody. Protein
579 preparations from cell lines treated with 1 μg/mL tunicamycin (Tm) or 5 mM dithiothreitol
580 (DTT) for 6 h were subjected to immunoblot analysis. Coomassie brilliant blue staining (CBB)
581 was used as a loading control.
582
583 **Supplemental Figure 4. Expression levels of acyltransferase genes in *crbzip1* mutants and**
584 **their parental strains under the ER stress.** Supports Figure 4C.
585 Cells were treated with 1 μg/mL tunicamycin (Tm) for the indicated periods. The RT-qPCR
586 results were normalized by the level of *RPL17* expression and the fold changes of expression
587 levels at 2 h and 6 h were determined relative to the levels at 0 h. Error bars represent standard
588 errors based on four biological replicates from two individual experiments. Statistical analysis
589 was carried out using Student's *t*-test (*, $p < 0.05$; **, $p < 0.01$) and the Wilcoxon rank sum test
590 (Supplemental Dataset 1).
591
592 **Supplemental Figure 5. Expression levels of *BTA1* and *CrDES* were recovered in the**

593 ***crbzip1-1C* and *crbzip1-2C* lines.** Supports Figures 4E and 5B.
594 Cells were treated with 1 μg/mL tunicamycin (Tm) for the indicated periods. The RT-qPCR
595 results were normalized by the level of *RPL17* expression and the fold changes of expression
596 levels at 6 h were determined relative to the levels at 0 h. Error bars represent standard errors
597 based on seven biological replicates from three individual experiments. Statistical analysis was
598 carried out using Student's *t*-test (*, $p < 0.05$; **, $p < 0.01$; NS, no significant change) and the
599 Wilcoxon rank sum test (Supplemental Dataset 1).
600
601 **Supplemental Figure 6. Fatty acid compositions of glycerolipids in *crbzip1* mutants**
602 **subjected to ER stress.** Supports Figure 4A.
603 The fatty acid composition in the glycerolipids: phosphatidylinositol (PI),
604 phosphatidylethanolamine (PE), phosphatidylglycerol (PG), sulfoquinovosyldiacylglycerol
605 (SQDG), monogalactosyldiacylglycerol (MGDG), digalactosyldiacylglycerol (DGDG), and
606 triacylglycerol (TAG). Lipids extracted from *crbzip1* mutants and their parental strains treated
607 with 1 μg/mL tunicamycin (Tm) for the indicated periods were analyzed using GC-FID. Error
608 bars represent standard errors based on three biological replicates. The statistical analysis is
609 described in Supplemental Dataset 2.
610
611 **Supplemental Figure 7. Isolation of *Chlamydomonas crdes1-1* and *crdes1-2* mutants.**
612 Supports Figure 6A.
613 (**A**) Schematic representation of insertion sites of the *APHVII* and *APHVIII* cassettes in the
614 genomic sequence of *CrDES* in *crdes* mutants. The positions of UTRs, exons, and introns are
615 indicated by dark-gray boxes, gray boxes, and lines, respectively. Arrows indicate primer
616 locations used to detect insertions in (B).
617 (**B**) Genotyping of the *crdes1-1* and *crdes1-2* mutants. Genomic DNA fragments were
618 amplified by PCR using the primer sets indicated in A.
619
620 **Supplemental Figure 8. Fatty acid compositions of glycerolipids in *crdes* mutants**
621 **subjected to ER stress.** Supports Figure 6B.
622 Total lipids were extracted from cells treated with 1 μg/mL tunicamycin (Tm) for the indicated
623 periods. Phosphatidylinositol (PI), phosphatidylethanolamine (PE), phosphatidylglycerol (PG),
624 sulfoquinovosyldiacylglycerol (SQDG), monogalactosyldiacylglycerol (MGDG),
625 digalactosyldiacylglycerol (DGDG), tracylglycerol (TAG). Yellow boxes indicate absence or
626 reduction of pinolenic acid in *crdes1-1* or *crdes1-2* mutants, respectively. Red boxes indicate

compensatory increases of alpha-linolenic acid in *crdes1* mutants. Error bars represent standard errors based on three biological replicates. Statistical analysis is described in Supplemental Dataset 3.

FIGURE LEGENDS

Figure 1. Identification of the transcription factor targeted by *Chlamydomonas* IRE1.

(**A**) Molecular phylogenetic analysis of the *Chlamydomonas* bZIP proteins and the *Arabidopsis* AtbZIP60 protein reported to be important for ER stress (Nagashima et al., 2011; Deng et al., 2011). The analysis was conducted in MEGA7 (Kumar et al., 2016), using the Maximum Likelihood method based on the JTT matrix-based model (Jones et al., 1992). The tree is drawn to scale, with branch lengths measured in number of substitutions per site.

(**B**) Unspliced *CrbZIP1* (*CrbZIP1u*) and spliced *CrbZIP1* (*CrbZIP1s*) detected using primers flanking the spliced region of *CrbZIP1* (arrows in C). Under the ER stress conditions imposed by 1 μg/mL tunicamycin (Tm), *CrbZIP1u* is spliced to *CrbZIP1s* in CC-4533 and C-9, but not in the *crire1* mutants, *crire1-1* and *crire1-2*. *Chlamydomonas* cells were incubated in TAP medium containing 1 μg/mL Tm.

(**C**) Schematic representations of *CrbZIP1u* mRNA and *CrbZIP1s* mRNA and primer locations used to detect splicing.

(**D**) Schematic representations of primary structures of CrbZIP1u and CrbZIP1s proteins. The bZIP motif and the transmembrane domain are indicated by bZIP and TM, respectively.

(**E**) Immunoblot analysis of CrbZIP1u and CrbZIP1s using anti-CrbZIP1 antibody. Protein preparations from cells treated with 1 μg/mL tunicamycin (Tm) or 5 mM dithiothreitol (DTT) for the indicated periods were subjected to immunoblot analysis. Coomassie brilliant blue staining (CBB) was used as a loading control.

(**F**) Cellular localization of CrbZIP1u-sGFP and CrbZIP1s-sGFP transiently expressed in *N. benthamiana* epidermal cells. The superfolder GFP (sGFP), ER marker (AtBiP1-tagRFP), DAPI (nuclear marker), and merged images of sGFP and ER marker, DAPI, and the bright field. Note that CrbZIP1u-sGFP mainly localizes to the ER membrane and CrbZIP1s-sGFP localizes to the nucleus. Typical images of each localization pattern were chosen from each of the 6 images analyzed. Bars = 50 μm.

Figure 2. Isolation and phenotypic analysis of *Chlamydomonas crbzip1* mutants.

(**A**) Schematic representation of the *APHVIII* cassettes inserted into the first exon of *CrbZIP1* in the *crbzip1* mutants. The positions of UTRs, exons, and introns are indicated by dark-gray

boxes, gray boxes, and lines, respectively.

(**B**) Photographs of cultures grown in control TAP medium or TAP medium containing 1 μg/mL Tm for the indicated periods.

(**C**) Cell numbers and viability of cells grown in the presence or absence of Tm. Propidium iodide (PI) was used to stain dead and damaged cells, and cells not stained with PI were considered healthy. Averages from four biological replicates from two individual experiments and their standard errors are shown.

(**D**) Confocal microscopy images of Nile red-stained cells grown in medium with 1 μg/mL Tm for 0, 6, 12, or 24 h. Images of chlorophyll autofluorescence were merged with those of Nile red fluorescence, which indicated lipid droplets.

Figure 3. Expression levels of ER stress marker genes in *crbzip1* mutants and their parental strains.

Cells were treated with 1 μg/mL tunicamycin (Tm) for the indicated periods. The RT-qPCR results were normalized by the level of *RPL17* expression and the fold changes of expression levels at 2 h and 6 h were determined relative to the levels at 0 h. Error bars represent standard errors based on four biological replicates from two individual experiments. Statistical analysis was carried out using a Student's *t*-test (*, $p < 0.05$; **, $p < 0.01$) and the Wilcoxon rank sum test (Supplemental Dataset 1).

Figure 4. ER-stress-induced lipid remodeling differs between the *crbzip1* mutant and their parental lines.

(**A**) Levels of fatty acids (FAs) in glycerolipids and the fatty acid composition of total fatty acids and of diacylglyceryltrimethylhomo-Ser (DGTS). Lipids extracted from *crbzip1* mutants and their parental strains treated with 1 μg/mL tunicamycin (Tm) for the indicated periods were analyzed using GC-FID. Error bars represent standard errors based on three biological replicates. Red box indicates TAG accumulation in *crbzip1* cells. Green box represents the induction of DGTS only in the parental strains. Blue boxes indicate the decreases of pinolenic acid in total FAs in *crbzip1* cells. Yellow boxes indicate the dramatic reductions of pinolenic acid in DGTS. phosphatidylinositol (PI), phosphatidylethanolamine (PE), phosphatidylglycerol (PG), sulfoquinovosyldiacylglycerol (SQDG), monogalactosyldiacylglycerol (MGDG), digalactosyldiacylglycerol (DGDG), and triacylglycerol (TAG). Statistical analysis was carried out using a Student's *t*-test (*, $p < 0.05$; **, $p < 0.01$, Supplemental Dataset 2), and the significant differences between the mutant and

the parental strain at the same time point are marked.

(**B**) Major TAG biosynthesis pathway mediated by DGTT1 in *Chlamydomonas*. DGTT1 is a critical enzyme for TAG synthesis in *Chlamydomonas*.

(**C**) Expression levels of *DGTT1* under ER stress. Cells were treated with 1 μg/mL Tm for the indicated periods. The RT-qPCR results were normalized by the level of *RPL17* expression and the fold changes of expression levels were determined relative to the levels at 0 h. Error bars represent standard errors based on four biological replicates at 0, 2, and 6 h. Statistical analysis was carried out using a Student's *t*-test (**, $p < 0.01$) and the Wilcoxon rank sum test (Supplemental Dataset 1).

(**D**) DGTS biosynthesis pathway mediated by BTA1 in *Chlamydomonas*. BTA1 is a critical enzyme for DGTS biosynthesis in *Chlamydomonas*.

(**E**) Expression level of *BTA1* in *Chlamydomonas* cells subjected to ER stress. Experimental conditions and data processing were the same as in (C).

(**F**) Yeast one-hybrid assay showing that CrbZIP1s interacts directly with the promoter region of *BTA1*. Yeast cells were spotted on medium containing SD-Leu-Ura-His with or without 3-AT with a series of 1:10 dilutions.

Figure 5. CrbZIP1s promotes the biosynthesis of pinolenic acid (18:3Δ5,9,12) under ER stress.

(**A**) C18 FA biosynthesis pathway in *Chlamydomonas*.

(**B**) Relative transcript abundance of desaturase genes after tunicamycin (Tm) treatment. Cells were treated with 1 μg/mL Tm for the indicated periods. The RT-qPCR results were normalized by the level of *RPL17* expression and the fold changes of expression levels were determined relative to the levels at 0 h. Error bars represent standard errors based on four biological replicates for 0, 2, and 6 h. Statistical analysis was carried out using a Student's *t*-test (*, $p < 0.05$; **, $p < 0.01$) and the Wilcoxon rank sum test (Supplemental Dataset 1).

(**C**) Yeast one-hybrid assay showing that CrbZIP1s interacts directly with the promoter region of *CrDES*. Yeast cells were spotted on medium containing SD-Leu-Ura-His with or without 3-AT with a series of 1:10 dilutions.

Figure 6. *crdes* knockdown mutants are hypersensitive to the ER stress imposed by tunicamycin treatment.

(**A**) Schematic representation of insertion sites of the *APHVII* and *APHVIII* cassettes in the genomic sequence of *CrDES* in *crdes* mutants. The positions of UTRs, exons, and introns are

indicated by dark-gray boxes, gray boxes, and lines, respectively.

(**B**) Levels of fatty acids (FAs) in glycerolipids and fatty acid composition of total fatty acids, phosphatidylethanolamine (PE), and diacylglyceryltrimethylhomo-Ser (DGTS). Total lipids were extracted from cells treated with 1 μg/mL tunicamycin (Tm) for the indicated periods. Blue arrows and green arrows indicate absence or reduction of pinolenic acid and coniferonic acid in *crdes1-1* and *crdes1-2* mutants, respectively. Yellow boxes indicate absence or reduction of pinolenic acid in *crdes1-1* or *crdes1-2* mutants, respectively. Red boxes indicate compensatory increases of alpha-linolenic acid in *crdes1* mutants. Error bars represent standard errors based on three biological replicates. Statistical analysis was performed as described in Supplemental Dataset 3.

(**C**) Growth of the indicated *Chlamydomonas* cell lines spotted on TAP medium supplemented with or without 0.2 μg/mL Tm with a series of 1:10 dilutions.

Figure 7. Proposed model for a mechanism of ER stress responses in *crbzip1* mutants and their parental lines in *Chlamydomonas*.

Left: In the parental lines, activated CrIRE1 splices Cr*bZIP1u* mRNA to produce *CrbZIP1s,* which is translated to CrbZIP1s. CrbZIP1s enters the nucleus, where it induces the expression of UPR genes and ER membrane lipid biosynthesis genes, such as *BTA1* and *CrDES*. The dimerization and phosphorylation of CrIRE1 are drawn based on reports in other organisms but have not been revealed in *Chlamydomonas.*

Right: The *crbzip1* mutation upregulates TAG biosynthesis from the fatty acids hydrolyzed from a major ER membrane lipid, DGTS, resulting in the formation of lipid droplets, which store TAGs.

Parsed Citations

Asset, G., Bauge, E., Wolff, R.L., Fruchart, J.C., and Dallongeville, J. (2001). Effects of dietary maritime pine seed oil on lipoprotein metabolism and atherosclerosis development in mice expressing human apolipoprotein B. Eur J Nutr 40, 268-274.
Pubmed: Author and Title
Google Scholar: Author Only Title Only Author and Title

Asset, G., Leroy, A., Bauge, E., Wolff, R.L., Fruchart, J.C., and Dallongeville, J. (2000). Effects of dietary maritime pine (Pinus pinaster)-seed oil on high-density lipoprotein levels and in vitro cholesterol efflux in mice expressing human apolipoprotein A-I. Br J Nutr 84, 353-360.
Pubmed: Author and Title
Google Scholar: Author Only Title Only Author and Title

Auton, M., Rosgen, J., Sinev, M., Holthauzen, L.M., and Bolen, D.W. (2011). Osmolyte effects on protein stability and solubility: a balancing act between backbone and side-chains. Biophys Chem 159, 90-99.
Pubmed: Author and Title
Google Scholar: Author Only Title Only Author and Title

Basseri, S., and Austin, R.C. (2012). Endoplasmic reticulum stress and lipid metabolism: mechanisms and therapeutic potential. Biochem Res Int 2012, 841362.
Pubmed: Author and Title
Google Scholar: Author Only Title Only Author and Title

Boyle, N.R., Page, M.D., Liu, B., Blaby, I.K., Casero, D., Kropat, J., Cokus, S.J., Hong-Hermesdorf, A., Shaw, J., Karpowicz, S.J., Gallaher, S.D., Johnson, S., Benning, C., Pellegrini, M., Grossman, A., and Merchant, S.S. (2012). Three acyltransferases and nitrogen-responsive regulator are implicated in nitrogen starvation-induced triacylglycerol accumulation in Chlamydomonas. J Biol Chem 287, 15811-15825.
Pubmed: Author and Title
Google Scholar: Author Only Title Only Author and Title

Deng, Y., Humbert, S., Liu, J.X., Srivastava, R., Rothstein, S.J., and Howell, S.H. (2011). Heat induces the splicing by IRE1 of a mRNA encoding a transcription factor involved in the unfolded protein response in Arabidopsis. Proc Natl Acad Sci U S A 108, 7247-7252.
Pubmed: Author and Title
Google Scholar: Author Only Title Only Author and Title

Gallaher, S.D., Fitz-Gibbon, S.T., Glaesener, A.G., Pellegrini, M., and Merchant, S.S. (2015). Chlamydomonas Genome Resource for Laboratory Strains Reveals a Mosaic of Sequence Variation, Identifies True Strain Histories, and Enables Strain-Specific Studies. Plant Cell 27, 2335-2352.
Pubmed: Author and Title
Google Scholar: Author Only Title Only Author and Title

Giroud, C., Gerber, A., and Eichenberger, W. (1988). Lipids of Chlamydomonas reinhardtii. Analysis of molecular species and intracellular site (s) of biosynthesis. Plant and Cell Physiology 29, 587-595.
Pubmed: Author and Title
Google Scholar: Author Only Title Only Author and Title

Han, J., and Kaufman, R.J. (2016). The role of ER stress in lipid metabolism and lipotoxicity. J Lipid Res 57, 1329-1338.
Pubmed: Author and Title
Google Scholar: Author Only Title Only Author and Title

Harris, E.H. (2001). Chlamydomonas as a Model Organism. Annu Rev Plant Physiol Plant Mol Biol 52, 363-406.
Pubmed: Author and Title
Google Scholar: Author Only Title Only Author and Title

Howell, S.H. (2013). Endoplasmic reticulum stress responses in plants. Annu Rev Plant Biol 64, 477-499.
Pubmed: Author and Title
Google Scholar: Author Only Title Only Author and Title

Jang, S., Yamaoka, Y., Ko, D., Kurita, T., Kim, K., Song, W.-Y., Hwang, J.U., Kang B.-H., Nishida, I., and Lee, Y. (2015) Characterization of a Chlamydomonas reinhardtii mutant defective in a maltose transporter. J. Plant Biol 58, 344.
Pubmed: Author and Title
Google Scholar: Author Only Title Only Author and Title

Jones, D.T., Taylor, W.R., and Thornton, J.M. (1992). The rapid generation of mutation data matrices from protein sequences. Comput Appl Biosci 8, 275-282.
Pubmed: Author and Title
Google Scholar: Author Only Title Only Author and Title

Kajikawa, M., Yamato, K.T., Kohzu, Y., Shoji, S., Matsui, K., Tanaka, Y., Sakai, Y., and Fukuzawa, H. (2006). A front-end desaturase from Chlamydomonas reinhardtii produces pinolenic and coniferonic acids by omega13 desaturation in methylotrophic yeast and tobacco. Plant Cell Physiol 47, 64-73.
Pubmed: Author and Title
Google Scholar: Author Only Title Only Author and Title

Kato, M., Sakai, M., Adachi, K., Ikemoto, H., and Sano, H. (1996). Distribution of betaine lipids in marine algae. Phytochemistry, 42, 1341-1345.
Pubmed: Author and Title
Google Scholar: Author Only Title Only Author and Title

Kim, H., Jang, S., Kim, S., Yamaoka, Y., Hong, D., Song, W.-Y., Nishida, I., Li-Beisson, Y., and Lee, Y. (2015). The small molecule fenpropimorph rapidly converts chloroplast membrane lipids to triacylglycerols in Chlamydomonas reinhardtii. Frontiers in microbiology 6.
Pubmed: Author and Title
Google Scholar: Author Only Title Only Author and Title

Kim, S., Kim, H., Ko, D., Yamaoka, Y., Otsuru, M., Kawai-Yamada, M., Ishikawa, T., Oh, H.M., Nishida, I., Li-Beisson, Y., and Lee, Y. (2013). Rapid induction of lipid droplets in Chlamydomonas reinhardtii and Chlorella vulgaris by Brefeldin A. PLoS One 8, e81978.
Pubmed: Author and Title
Google Scholar: Author Only Title Only Author and Title

Kimata, Y., and Kohno, K. (2011). Endoplasmic reticulum stress-sensing mechanisms in yeast and mammalian cells. Curr Opin Cell Biol 23, 135-142.
Pubmed: Author and Title
Google Scholar: Author Only Title Only Author and Title

Kumar, S., Stecher, G., and Tamura, K. (2016). MEGA7: Molecular Evolutionary Genetics Analysis Version 7.0 for Bigger Datasets. Mol Biol Evol 33, 1870-1874.
Pubmed: Author and Title
Google Scholar: Author Only Title Only Author and Title

Lee, J.W., Lee, K.W., Lee, S.W., Kim, I.H., and Rhee, C. (2004). Selective increase in pinolenic acid (all-cis-5,9,12-18:3) in Korean pine nut oil by crystallization and its effect on LDL-receptor activity. Lipids 39, 383-387.
Pubmed: Author and Title
Google Scholar: Author Only Title Only Author and Title

Li, X., Zhang, R., Patena, W., Gang, S.S., Blum, S.R., Ivanova, N., Yue, R., Robertson, J.M., Lefebvre, P.A., Fitz-Gibbon, S.T., Grossman, A.R., and Jonikas, M.C. (2016). An Indexed, Mapped Mutant Library Enables Reverse Genetics Studies of Biological Processes in Chlamydomonas reinhardtii. Plant Cell 28, 367-387.
Pubmed: Author and Title
Google Scholar: Author Only Title Only Author and Title

Listenberger, L.L., Han, X., Lewis, S.E., Cases, S., Farese, R.V., Jr., Ory, D.S., and Schaffer, J.E. (2003). Triglyceride accumulation protects against fatty acid-induced lipotoxicity. Proc Natl Acad Sci U S A 100, 3077-3082.
Pubmed: Author and Title
Google Scholar: Author Only Title Only Author and Title

Mandl, J., Meszaros, T., Banhegyi, G., and Csala, M. (2013). Minireview: endoplasmic reticulum stress: control in protein, lipid, and signal homeostasis. Mol Endocrinol 27, 384-393.
Pubmed: Author and Title
Google Scholar: Author Only Title Only Author and Title

Mene-Saffrane, L., Dubugnon, L., Chetelat, A., Stolz, S., Gouhier-Darimont, C., and Farmer, E.E. (2009). Nonenzymatic oxidation of trienoic fatty acids contributes to reactive oxygen species management in Arabidopsis. J Biol Chem 284, 1702-1708.
Pubmed: Author and Title
Google Scholar: Author Only Title Only Author and Title

Merchant, S.S., Kropat, J., Liu, B., Shaw, J., and Warakanont, J. (2012). TAG, you're it! Chlamydomonas as a reference organism for understanding algal triacylglycerol accumulation. Curr Opin Biotechnol 23, 352-363.
Pubmed: Author and Title
Google Scholar: Author Only Title Only Author and Title

Moellering, E.R., Muthan, B., and Benning, C. (2010). Freezing tolerance in plants requires lipid remodeling at the outer chloroplast membrane. Science 330, 226-228.
Pubmed: Author and Title
Google Scholar: Author Only Title Only Author and Title

Moore, T.S., Du, Z., and Chen, Z. (2001). Membrane lipid biosynthesis in Chlamydomonas reinhardtii. In vitro biosynthesis of diacylglyceryltrimethylhomoserine. Plant Physiol 125, 423-429.
Pubmed: Author and Title
Google Scholar: Author Only Title Only Author and Title

Nagashima, Y., Mishiba, K., Suzuki, E., Shimada, Y., Iwata, Y., and Koizumi, N. (2011). Arabidopsis IRE1 catalyses unconventional splicing of bZIP60 mRNA to produce the active transcription factor. Sci Rep 1, 29.
Pubmed: Author and Title
Google Scholar: Author Only Title Only Author and Title

Nakagawa, T., Suzuki, T., Murata, S., Nakamura, S., Hino, T., Maeo, K., Tabata, R., Kawai, T., Tanaka, K., Niwa, Y., Watanabe, Y., Nakamura, K., Kimura, T., and Ishiguro, S. (2007). Improved Gateway binary vectors: high-performance vectors for creation of fusion

constructs in transgenic analysis of plants. Biosci Biotechnol Biochem 71, 2095-2100.
Pubmed: Author and Title
Google Scholar: Author Only Title Only Author and Title

Nakagawa, T., Nakamura, S., Tanaka, K., Kawamukai, M., Suzuki, T., Nakamura, K., Kimura, T., and Ishiguro, S. (2008). Development of R4 gateway binary vectors (R4pGWB) enabling high-throughput promoter swapping for plant research. Biosci Biotechnol Biochem 72, 624-629.
Pubmed: Author and Title
Google Scholar: Author Only Title Only Author and Title

Pasman, W.J., Heimerikx, J., Rubingh, C.M., van den Berg, R., O'Shea, M., Gambelli, L., Hendriks, H.F., Einerhand, A.W., Scott, C., Keizer, H.G., and Mennen, L.I. (2008). The effect of Korean pine nut oil on in vitro CCK release, on appetite sensations and on gut hormones in post-menopausal overweight women. Lipids Health Dis 7, 10.
Pubmed: Author and Title
Google Scholar: Author Only Title Only Author and Title

Perez-Martin, M., Perez-Perez, M.E., Lemaire, S.D., and Crespo, J.L. (2014). Oxidative stress contributes to autophagy induction in response to endoplasmic reticulum stress in Chlamydomonas reinhardtii. Plant Physiol 166, 997-1008.
Pubmed: Author and Title
Google Scholar: Author Only Title Only Author and Title

Riekhof, W.R., Sears, B.B., and Benning, C. (2005). Annotation of genes involved in glycerolipid biosynthesis in Chlamydomonas reinhardtii: discovery of the betaine lipid synthase BTA1Cr. Eukaryot Cell 4, 242-252.
Pubmed: Author and Title
Google Scholar: Author Only Title Only Author and Title

Rogers, R.W., and Clifford, H.T. (2006). The taxonomic and evolutionary significance of leaf longevity. New Phytologist 123, 811-821.
Pubmed: Author and Title
Google Scholar: Author Only Title Only Author and Title

Ron, D., and Walter, P. (2007). Signal integration in the endoplasmic reticulum unfolded protein response. Nat Rev Mol Cell Biol 8, 519-529.
Pubmed: Author and Title
Google Scholar: Author Only Title Only Author and Title

Schuck, S., Prinz, W.A., Thorn, K.S., Voss, C., and Walter, P. (2009). Membrane expansion alleviates endoplasmic reticulum stress independently of the unfolded protein response. J Cell Biol 187, 525-536.
Pubmed: Author and Title
Google Scholar: Author Only Title Only Author and Title

Siaut, M., Cuine, S., Cagnon, C., Fessler, B., Nguyen, M., Carrier, P., Beyly, A., Beisson, F., Triantaphylides, C., Li-Beisson, Y., and Peltier, G. (2011). Oil accumulation in the model green alga Chlamydomonas reinhardtii: characterization, variability between common laboratory strains and relationship with starch reserves. BMC Biotechnol 11, 7.
Pubmed: Author and Title
Google Scholar: Author Only Title Only Author and Title

Sievers, F., Wilm, A., Dineen, D., Gibson, T.J., Karplus, K., Li, W., Lopez, R., McWilliam, H., Remmert, M., Soding, J., Thompson, J.D., and Higgins, D.G. (2011). Fast, scalable generation of high-quality protein multiple sequence alignments using Clustal Omega. Mol Syst Biol 7, 539.
Pubmed: Author and Title
Google Scholar: Author Only Title Only Author and Title

Song, W.Y., Martinoia, E., Lee, J., Kim, D., Kim, D.Y., Vogt, E., Shim, D., Choi, K.S., Hwang, I., and Lee, Y. (2004). A novel family of cys-rich membrane proteins mediates cadmium resistance in Arabidopsis. Plant Physiol 135, 1027-1039.
Pubmed: Author and Title
Google Scholar: Author Only Title Only Author and Title

Sparkes, I.A., Runions, J., Kearns, A., and Hawes, C. (2006). Rapid, transient expression of fluorescent fusion proteins in tobacco plants and generation of stably transformed plants. Nat Protoc 1, 2019-2025.
Pubmed: Author and Title
Google Scholar: Author Only Title Only Author and Title

Sriburi, R., Bommiasamy, H., Buldak, G.L., Robbins, G.R., Frank, M., Jackowski, S., and Brewer, J.W. (2007). Coordinate regulation of phospholipid biosynthesis and secretory pathway gene expression in XBP-1(S)-induced endoplasmic reticulum biogenesis. J Biol Chem 282, 7024-7034.
Pubmed: Author and Title
Google Scholar: Author Only Title Only Author and Title

Withington, J.M., Reich, P.B., Oleksyn, J., and Eissenstat, D.M. (2006). COMPARISONS OF STRUCTURE AND LIFE SPAN IN ROOTS AND LEAVES AMONG TEMPERATE TREES. Ecological Monographs 76, 381-397.
Pubmed: Author and Title
Google Scholar: Author Only Title Only Author and Title

Yamano, T., Sato, E., Iguchi, H., Fukuda, Y., and Fukuzawa, H. (2015). Characterization of cooperative bicarbonate uptake into

chloroplast stroma in the green alga Chlamydomonas reinhardtii. Proc Natl Acad Sci U S A 112, 7315-7320.
Pubmed: Author and Title
Google Scholar: Author Only Title Only Author and Title

Yamaoka, Y., Choi, B.Y., Kim, H., Shin, S., Kim, Y., Jang, S., Song, W.Y., Cho, C.H., Yoon, H.S., Kohno, K., and Lee, Y. (2018). Identification and functional study of the endoplasmic reticulum stress sensor IRE1 in Chlamydomonas reinhardtii. Plant J 94, 91-104.
Pubmed: Author and Title
Google Scholar: Author Only Title Only Author and Title

Yamaoka, Y., Yu, Y., Mizoi, J., Fujiki, Y., Saito, K., Nishijima, M., Lee, Y., and Nishida, I. (2011). PHOSPHATIDYLSERINE SYNTHASE1 is required for microspore development in Arabidopsis thaliana. Plant J 67, 648-661.
Pubmed: Author and Title
Google Scholar: Author Only Title Only Author and Title

Yanagitani, K., Imagawa, Y., Iwawaki, T., Hosoda, A., Saito, M., Kimata, Y., and Kohno, K. (2009). Cotranslational targeting of XBP1 protein to the membrane promotes cytoplasmic splicing of its own mRNA. Mol Cell 34, 191-200.
Pubmed: Author and Title
Google Scholar: Author Only Title Only Author and Title

Yanagitani, K., Kimata, Y., Kadokura, H., and Kohno, K. (2011). Translational pausing ensures membrane targeting and cytoplasmic splicing of XBP1u mRNA. Science 331, 586-589.
Pubmed: Author and Title
Google Scholar: Author Only Title Only Author and Title

Zhou, H., and Liu, R. (2014). ER stress and hepatic lipid metabolism. Front Genet 5, 112.
Pubmed: Author and Title
Google Scholar: Author Only Title Only Author and Title

Zoeller, M., Stingl, N., Krischke, M., Fekete, A., Waller, F., Berger, S., and Mueller, M.J. (2012). Lipid profiling of the Arabidopsis hypersensitive response reveals specific lipid peroxidation and fragmentation processes: biogenesis of pimelic and azelaic acid. Plant Physiol 160, 365-378.
Pubmed: Author and Title
Google Scholar: Author Only Title Only Author and Title